Cerebrospinal Fluid Research

BioMed Central

Research

Open Access

Activation of adenosine A_{2B} receptors enhances ciliary beat frequency in mouse lateral ventricle ependymal cells

Jonathan R Genzen[1,4], Dan Yang[3], Katya Ravid[3] and Angelique Bordey*[2]

Address: [1]Department of Laboratory Medicine, Yale University School of Medicine, New Haven, CT 06520-8082, USA, [2]Departments of Neurosurgery & Cellular and Molecular Physiology, Yale University School of Medicine, New Haven, CT 06520-8082, USA, [3]Departments of Biochemistry, Medicine, and Whitaker Cardiovascular Institute, Boston University School of Medicine, Boston, MA 02118, USA and [4]Department of Pathology and Laboratory Medicine, Weill Cornell Medical College, New York-Presbyterian Hospital, New York, NY 10065, USA

Email: Jonathan R Genzen - jrg9010@med.cornell.edu; Dan Yang - yangdan@bu.edu; Katya Ravid - ravid@biochem.bumc.bu.edu; Angelique Bordey* - angelique.bordey@yale.edu

* Corresponding author

Published: 18 November 2009

Cerebrospinal Fluid Research 2009, **6**:15 doi:10.1186/1743-8454-6-15

Received: 20 August 2009
Accepted: 18 November 2009

This article is available from: http://www.cerebrospinalfluidresearch.com/content/6/1/15

Abstract

Background: Ependymal cells form a protective monolayer between the brain parenchyma and cerebrospinal fluid (CSF). They possess motile cilia important for directing the flow of CSF through the ventricular system. While ciliary beat frequency in airway epithelia has been extensively studied, fewer reports have looked at the mechanisms involved in regulating ciliary beat frequency in ependyma. Prior studies have demonstrated that ependymal cells express at least one purinergic receptor ($P2X_7$). An understanding of the full range of purinergic receptors expressed by ependymal cells, however, is not yet complete. The objective of this study was to identify purinergic receptors which may be involved in regulating ciliary beat frequency in lateral ventricle ependymal cells.

Methods: High-speed video analysis of ciliary movement in the presence and absence of purinergic agents was performed using differential interference contrast microscopy in slices of mouse brain (total number of animals = 67). Receptor identification by this pharmacological approach was corroborated by immunocytochemistry, calcium imaging experiments, and the use of two separate lines of knockout mice.

Results: Ciliary beat frequency was enhanced by application of a commonly used $P2X_7$ agonist. Subsequent experiments, however, demonstrated that this enhancement was observed in both $P2X_7^{+/+}$ and $P2X_7^{-/-}$ mice and was reduced by pre-incubation with an ecto-5'-nucleotidase inhibitor. This suggested that enhancement was primarily due to a metabolic breakdown product acting on another purinergic receptor subtype. Further studies revealed that ciliary beat frequency enhancement was also induced by adenosine receptor agonists, and pharmacological studies revealed that ciliary beat frequency enhancement was primarily due to A_{2B} receptor activation. A_{2B} expression by ependymal cells was subsequently confirmed using $A_{2B}^{-/-}$/β-galactosidase reporter gene knock-in mice.

Conclusion: This study demonstrates that A_{2B} receptor activation enhances ciliary beat frequency in lateral ventricle ependymal cells. Ependymal cell ciliary beat frequency regulation may play an important role in cerebral fluid balance and cerebrospinal fluid dynamics.

Background

The cerebral ventricles are lined by a layer of ciliated ependymal cells that play an important role in cerebral fluid balance [1]. It has been estimated that each ependymal cell possesses 20-30 motile cilia, which are 8-20 μm in length with a 9 + 2 microtubule structure. Their ciliary tufts are organized in a manner consistent with the direction of cerebrospinal fluid (CSF) flow [2]. Abnormalities in ciliogenesis or ciliary function are frequently associated with hydrocephalus [3-11], and ependymal denudation can be observed in cases of communicating hydrocephalus [12]. Despite the increased recognition that ependymal cells are important for regulating CSF dynamics, only a few reports have specifically looked at the extracellular signaling mechanisms involved ependymal cell ciliary beat frequency modulation.

Nelson and Wright (1974) noted enhancement of frog brain ependymal ciliary beat frequency by ATP (adenosine 5'-triphosphate), cAMP (adenosine 3',5'-cyclic monophosphate), theophylline, and acetylcholine, as well as decreases in ciliary beat frequency by a number of other agents, using an *in vitro* preparation [13]. A later study by Nguyen *et al*. (2001) observed an ATP-mediated decrease in ciliary beat frequency, as well as a serotonin-mediated increase, in 4th ventricle ependymal cells in cultured rat brain slices and acutely isolated ependymal cells [14]. Finally, reports from O'Callaghan *et al*. have demonstrated that both hydrogen peroxide and bacterial pneumolysin inhibit ciliary beat frequency in rat brain ependymal cells [15,16].

Recent work from our laboratory demonstrated that the purinergic $P2X_7$ receptor is widely expressed on ependymal cells [17]. Furthermore, receptor activation leads to increases in intracellular calcium ($[Ca^{2+}]_i$) both in the soma and cilia. Working under the hypothesis that the $P2X_7$ receptor may be involved in regulating ciliary beat frequency, we have conducted experiments using high-speed video capture and differential interference contrast (DIC) microscopy to investigate potential modulation of ciliary beat frequency by purinergic agonists. These experiments have demonstrated, however, that the adenosine A_{2B} receptor is primarily responsible for ciliary beat frequency enhancement by these agents. Further experiments using $A_{2B}^{-/-}$/β-galactosidase reporter gene knock-in mice confirmed this observation and also demonstrated a residual $P2X_7$-mediated component to ciliary beat frequency enhancement.

Methods

Slice preparation

Research protocols were approved by the Yale University Institutional Animal Care and Use Committee (approval #A3230-01). C57BL/6 mice (n = 48; Jackson Laboratories, Bar Harbor, ME, USA), CD1 mice (n = 7; Charles River Laboratories, Wilmington, MA, USA), $P2X_7$ knockout mice (n = 5; *P2rx7*^{tm1Gab}, Jackson Laboratories, [18]), and A_{2B} knockout mice (n = 7, [19]) were used for the present experiments. Mean age of animals was 24.3 ± 1.0 days (range 13-39). Animals were anesthetized with pentobarbital, 50 mg/kg, intraperitoneal (IP); after craniotomy and dissection, horizontal brain slices (250-300 μm) were prepared in chilled (4°C) dissection solution (in mM): 83 NaCl, 73 sucrose, 2.5 KCl, 2.7 $MgCl_2$, 1.7 $CaCl_2$, 1.2 NaH_2PO_4, 10 glucose, 26 $NaHCO_3$, pH 7.4 and bubbled with 95% O_2/5% CO_2 using a series 1000 Vibratome (The Vibratome Company, St. Louis, MO, USA). Slices were incubated for >1 h in artificial CSF (aCSF) at room temperature (in mM): 125 NaCl, 2.5 KCl, 1 $MgCl_2$, 2 $CaCl_2$, 1.25 NaH_2PO_4, 10 glucose, and 26 $NaHCO_3$, pH 7.4 and bubbled with 95% O_2/5% CO_2. Slices were transferred to a recording chamber and superfused (~1 ml/min) with aCSF and bubbled with 95% O_2/5% CO_2 at room temperature. Experiments were performed on an upright microscope (Olympus BX51WI; Olympus, Center Valley, PA, USA) under phase-contrast optics (60× objective, NA 0.9) and a 2× teleconverter. Ciliated ependymal cells were visually identified along the subventricular zone (SVZ) border lining the lateral surface of the lateral ventricles (e.g. Fig. 1A). Agonists and antagonists were bath applied, and only one exposure or experimental condition was permitted per slice. After preliminary time course experiments (see Fig. 1B), ciliary beat frequency measurements were analyzed at baseline then five min after agonist application unless otherwise indicated. Antagonists and inhibitors were always pre-applied (range 4-15 min), depending on the site of action (extracellular versus intracellular), and our prior experience using these agents in patch clamp experiments [17]; they were also present during agonist applications (for antagonist experiments only) to decrease the possibility of antagonist washout.

Ciliary Beat Frequency Analysis

Ciliary beat frequency on lateral ventricle ependymal cells was analyzed using modifications of a previously published approach [15]. High-speed video acquisition of ciliary beat frequency was performed using a Pioneer A640-210 gm GigE camera (Basler Vision Technologies, Exton, PA, USA) with StreamPix3 software (Norpix Inc., Montreal, Quebec, Canada). One-sec videos along the ependymal wall were digitally acquired to a Dell Computer (Round Rock, TX, USA) at 200 frames per sec (fps). Files were converted to multi-TIFF stacks of 200 images and imported into ImageJ (NIH, Bethesda, MD, USA), where the stacks were re-sliced along a line placed across the ciliary tuft, thus creating pseudo-line scans. Ciliary beat frequency was calculated by measuring peak-to-peak intervals of periodicity evident in the pseudo-line scan

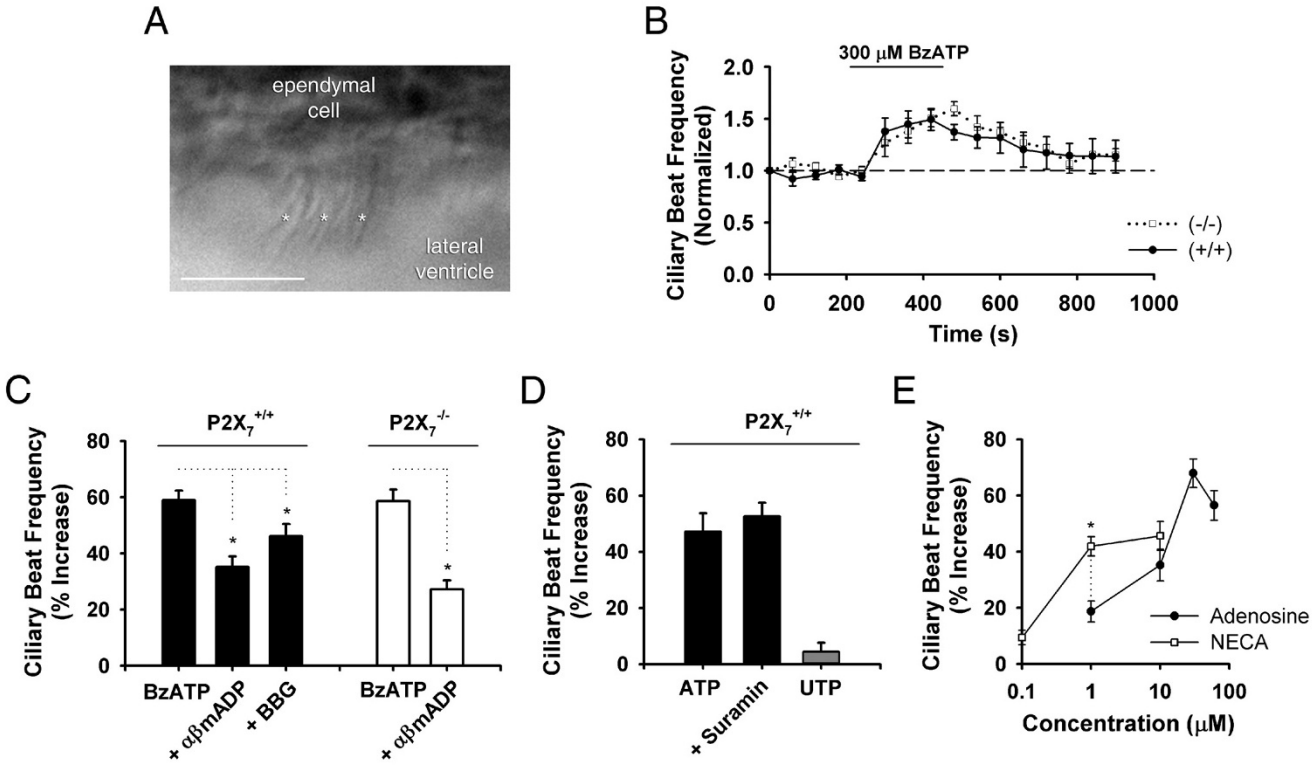

Figure 1

Purinergic enhancement of ciliary beat frequency is observed in both $P2X_7^{+/+}$ and $P2X_7^{-/-}$ mice. (*A*) DIC image of an ependymal cell. (Bar = 12 μm) Cilia are noted (*). (*B*) Beat frequency (normalized) during 300 μM BzATP application in slices from $P2X_7^{+/+}$ (filled circles/solid line; n = 5) and $P2X_7^{-/-}$ (open squares/dotted line; n = 4) mice. Responses from $P2X_7^{+/+}$ and $P2X_7^{-/-}$ animals were not significantly different. (*C*) Beat frequency (% increase) in slices from $P2X_7^{+/+}$ (n = 5) and $P2X_7^{-/-}$ (n = 4) mice after 5 min 300 μM BzATP application. Decreases ($P < 0.05$) were observed in the presence of the ecto-5'-nucleotidase inhibitor αβmADP (50 μM) in $P2X_7^{+/+}$ (n = 6) and $P2X_7^{-/-}$ (n = 6) mice. BBG significantly decreased BzATP-induced enhancement in $P2X_7^{+/+}$ mice (n = 4). (*D*) Beat frequency (% increase) in $P2X_7^{+/+}$ mice during application of 100 μM ATP ($P < 0.05$ compared to no drug control; n = 4). The P2Y receptor antagonist suramin (200 μM; n = 5) did not significantly reduce enhancement seen with 100 μM ATP. Beat frequency was not enhanced by the $P2Y_2/P2Y_4$ agonist UTP (100 μM; n = 2). (*E*) Beat frequency enhancement with increasing concentrations of adenosine (filled circles; n = 4-5) and NECA (open squares; n = 4-8). A significant difference was observed between NECA and adenosine at 1 μM. *: $P < 0.05$ for all panels, data are means ± SEM. The *n* value indicates number of slices tested.

and derived from the following equation, with each pixel representing 1/200 of a second.

$$\text{Ciliary beat frequency} = 1/(\#\text{ of pixels in wave period} / 200) \quad (1)$$

Ten periods were measured for each video, representing cilia from 3-6 ependymal cells on average. Analysis was conducted blinded to experimental conditions and with randomized file names and chronology, thus decreasing potential bias. Ciliary beat frequency data from pharmacological studies are presented using the following two equations:

$$\text{Ciliary beat frequency (normalized)} = \text{beat frequency during agonist application} \div \text{beat frequency at baseline} \quad (2)$$

$$\text{Ciliary beat frequency (\% increase)} = ((\text{beat frequency during agonist application} \div \text{beat frequency at baseline})-1)*100 \quad (3)$$

Comparison of our methodology to separate manual counting of ciliary beat frequency in the 1 sec video playback, as well as repeat analysis of duplicate files (with randomized names and chronology), yielded a strong correlation as determined by linear regression ($r^2 = 0.905$ and 0.95 respectively; data not shown).

Immunocytochemistry

Immunocytochemistry was performed according to previously described protocols [17]. Briefly, animals were anesthetized with pentobarbital (50 mg/kg, IP), then fixed by transcardiac perfusion with phosphate buffered saline (PBS; 20 ml) followed by 4% paraformaldehyde (Electron Microscopy Sciences, Hatfield, PA, USA) in PBS (30 ml). The brains were removed and post-fixed in 4% paraformaldehyde in PBS (24 h, 4°C). 100 μm slices were then made using a series 1000 Vibratome. Slices were washed with 0.05 M tris base in 9% NaCl at pH 7.4 (TBS), permeabilized in TBS + 0.1% Triton X-100 (TBST), blocked in TBST + 10% normal donkey serum, and then incubated overnight with primary antibody at 4°C. Antibodies included 1:100 rabbit anti-S100β (Sigma, St. Louis, MO, USA), 1:1000 mouse anti-β-galactosidase (Sigma), 1:100 mouse anti-A_{2A} (Upstate, Millipore, Billerica, MA, USA), and 1:100 rabbit anti-A_{2B} (Santa Cruz Biotechnology, Santa Cruz, CA, USA). After washing (3 × 45 min in TBST), slices were incubated 2 h at room temperature in secondary antibody solution (donkey, Alexa Fluor® 488, 594, 633, and/or 647; Invitrogen, Carlsbad, CA, USA). After 3 × 30 minute washes in TBS they were mounted and coverslipped with Prolong Gold Antifade Reagent (Invitrogen) with or without 1:1000 DAPI (2-(4-amidinophenyl)-6-indolecarbamidine dihydrochloride; Invitrogen).

β-galactosidase (β-gal) expression analysis in A_{2B} reporter mice

β-gal expression in $A_{2B}^{-/-}$/β-gal reporter gene knock-in mice was studied according to a previously published protocol [19]. Mice were anesthetized with isoflurane, perfused with 20 ml PBS through the left heart ventricle, and perfusion fixed with 30 ml 2% paraformaldehyde in PBS. Brains were removed, cut into 2 mm coronal sections containing intact lateral ventricular walls, and stained for β-gal activity using X-gal staining solution: 5 mM $K_3Fe(CN)_6$, 5 mM $K_4Fe(CN)_6 \cdot 2$ mM $MgCl_2$ in PBS, with a final concentration of 1 mg/ml 5-bromo-4-chloro-3-indolyl-β-D-galactopyranoside (X-gal, American Bioanalytical; Nantick, MA, USA), then incubated at 37° for 6-12 h, rinsed in PBS, and stored in 4% paraformaldehyde. Sections were embedded in low melting point agarose (American Bioanalytical), resectioned to 100 μm, and mounted directly onto slides or used for subsequent immunocytochemistry as previously described.

Calcium imaging

Acute mouse brain slices were loaded with the Ca^{2+}-sensitive dye Fluo-4 AM (Invitrogen; 4 μM in dimethyl sulfoxide (DMSO) with 20% Pluronic F-127) using ependyma-directed applications by a Picospritzer II (1-2 psi; Parker Instrumentation, Cleveland, OH, USA). Slices were washed for a minimum of 10 min before recording. The Ca^{2+} imaging system consisted of a confocal laser scanning microscope (Olympus) with a 60× water objective (NA 0.9) and Fluoview software (Olympus). Agonists in Ca^{2+} imaging experiments were focally applied using a Picospritzer II (as above). Calcium data were analyzed using the Calsignal program [20].

Genotyping

WT C57BL/6 ($P2X7^{+/+}$), $P2X7^{-/-}$, and $A_{2B}^{-/-}$/β-gal mice were maintained as separate, homozygous colonies. Genotyping was performed on all animals used in knockout-related experiments to survey for any potential errors in animal husbandry [17,19].

The $A_{2B}^{-/-}$/β-gal mice were previously bred onto a pure C57BL/6J background strain [21]. $P2X7^{-/-}$ mice were previously backcrossed to C57BL/6 mice for 7 generations (Jackson Laboratories, JAX® Mice Database; http://jaxmice.jax.org). We cannot exclude the possibility, however, that additional genetic variation exists between the C57BL/6 ($P2X7^{+/+}$), $P2X7^{-/-}$, and $A_{2B}^{-/-}$/β-gal strains.

Reagents

Salts used for aCSF solution, as well as adenosine, αβmADP, ATP, BzATP, dipyridamole, NBMPR, phloridzin, and UTP were purchased from Sigma. CGS 21680, IB-MECA, 2'MeCCPA, MRS 1754, NECA, and PSB 603 were purchased from Tocris (Ellisville, MO, USA). A list of all drugs used in the present experiments is included in Table 1.

Statistics

Data were analyzed and presented in SigmaPlot 8.0 (SPSS, Chicago, IL, USA). Statistical significance was determined using the Student's t-test ($P < 0.05$). Data are presented as mean ± standard error of the mean (SEM) unless otherwise indicated. Reported *n* values refer to the number of slices tested (with each slice including 10 ciliary beat frequency measurements; see above).

Results

Purinergic enhancement of ciliary beat frequency is present in $P2X7^{+/+}$ and $P2X7^{-/-}$ mice and is induced by non-selective adenosine receptor agonist

Given our prior demonstration of ciliary (and somatic) localization of $P2X_7$ receptors on lateral ventricle ependymal cells [17], we first sought to determine whether BzATP (a commonly used $P2X_7$ agonist) was also able to induce changes in ciliary beat frequency. Ciliated ependymal cells were visualized in horizontal mouse brain slices using high-speed DIC microscopy (Fig. 1A; see *Methods* for ciliary beat frequency calculations). Average baseline ciliary beat frequency was 11.4 ± 0.2 Hz (n = 160) in wild-type mice. While 300 μM BzATP (Fig. 1B) was able to increase ciliary beat frequency in C57BL/6 wild-type ($P2X_7^{+/+}$) mice, a similar increase was also observed in

Table 1: List of drugs used

Abbreviation	Full Name	Site of Action*
αβmADP	Adenosine 5'-(α,β-methylene)diphosphate	Ecto-5'-nucleotidase inhibitor
Adenosine	9-β-D-Ribofuranosyladenine	Nonselective adenosine receptor agonist
ATP	Adenosine 5'-triphosphate	P2 purinergic agonist
BBG	Brilliant blue G	$P2X_7$ receptor antagonist
BzATP	2'(3')-*O*-(4-benzoylbenzoyl)adenosine 5'-triphosphate triethylammonium salt	P2X purinergic agonist; more potent than ATP at $P2X_7$ receptors
CGS-21680	4-[2-[[6-Amino-9-(*N*-ethyl-b-D-ribofuranuronamidosyl)-9*H*-purin-2-yl]amino]ethyl]benzenepropanoic acid hydrochloride	A_{2A} adenosine receptor agonist
Dipyridamole	2,6-Bis(Diethanolamino)-4,8-dipiperidinopyrimido [5,4-d] pyrimidine	Equlibrative nucleoside transporter inhibitor
IB-MECA	1-Deoxy-1-[6-[[(3-iodophenyl)methyl]amino]-9*H*-purin-9-y l]-*N*-methyl-b-D-ribofuranuronamide	Selective A_3 adenosine receptor agonist
2'MeCCPA	2-Chloro-*N*-cyclopentyl-2'-methyladenosine	Selective A_1 adenosine receptor agonist
MRS 1754	*N*-(4-cyanophenyl)-2-[4-(2,3,6,7-tetrahydro-2,6-dioxo-1,3-dipropyl-1*H*-purin-8-yl)phenoxy]-acetamide	Selective adenosine A_{2B} receptor antagonist
NBMPR	S-(4-Nitrobenzyl)-6-thioinosine	Equilibrative nucleoside transporter 1 inhibitor
NECA	5'-*N*-ethylcarboxamidoadenosine	Nonselective adenosine receptor agonist.
Phloridzin	Phloretin 2'-β-D-glucopyranoside	Concentrative nucleoside transporter inhibitor
PSB 603	8-[4-[4-(4-Chlorophenzyl)piperazide-1-sulfonyl)phenyl]]-1-propylxanthine	Selective adenosine A_{2B} receptor antagonist
Suramin	8,8'-[Carbonylbis[imino-3,1-phenylenecarbonylimino(4-me thyl-3,1-phenylene)carbonylimino]]bis-1,3,5-naphthalene trisulfonic acid hexasodium salt	P2 antagonist (with broad subtype selectivity)
UTP	Uridine 5'-triphosphate	$P2Y_2$/$P2Y_4$ receptor agonist

* Selectivity depends on the concentration tested. Non-purinergic activities may also be present.

$P2X_7^{-/-}$ animals. Fig. 1C shows the % increase after a 5 min application of 300 μM BzATP in $P2X_7^{+/+}$ mice (58.9 ± 3.4%) and in $P2X_7^{-/-}$ mice (58.6 ± 4.1%). These responses were not significantly different.

Preincubation with 100 nM brilliant blue G (BBG; a $P2X_7$ antagonist), however, did result in a partial inhibition of BzATP-induced beat frequency enhancement in $P2X_7^{+/+}$ animals (Fig. 1C; 46.1 ± 4.4%). This suggests that $P2X_7$ may contribute only a minor component to BzATP-induced enhancement in wild-type mice. A significant decrease in BzATP-induced enhancement, $P < 0.05$, however, was also observed when the ecto-5'-nucleotidase inhibitor αβmADP (50 μM, [22]) was present in the bath solution for both $P2X_7^{+/+}$ mice (35.1 ± 3.8%) and $P2X_7^{-/-}$ mice (27.2 ± 3.2%, Fig. 1C) thus providing evidence that enhancement may be dependent on a metabolic breakdown product of BzATP.

To determine if either P2Y receptors or adenosine receptors are involved in ciliary beat frequency enhancement, experiments were performed using ATP, UTP, and a P2Y antagonist suramin (Fig. 1D), as well as adenosine and the non-selective adenosine receptor agonist 5'-*N*-ethylcarboxamidoadenosine (NECA) (Fig. 1E). While beat frequency increase was observed during 100 μM ATP

applications (47.1 ± 6.6%), pre-incubation with the commonly used P2Y receptor antagonist suramin (200 μM) did not reduce the ATP-induced increase in frequency (Fig. 1D; 52.6 ± 4.8%). Furthermore, application of the $P2Y_2/P2Y_4$ agonist UTP (Fig. 1D, 100 μM, 4.4 ± 3.2%) did not induce a significant change in baseline frequency, arguing against a role for these receptors in the ATP-induced effect. Dose-response experiments (Fig. 1E) showed that beat frequency increased with adenosine (1 μM, 18.7 ± 3.7%, n = 5; 10 μM, 35.1 ± 5.6%, n = 5; 30 μM, 67.9 ± 5.1%, n = 5; 60 μM, 56.5 ± 5.3%, n = 4) and with NECA (100 nM, 9.4 ± 2.6%, n = 5; 1 μM, 41.9 ± 3.4%, n = 8; 10 μM, 45.6 ± 5.1%, n = 4), and that NECA had a greater potency than adenosine.

A_{2B} receptors mediate adenosine and NECA-induced ciliary beat frequency enhancement

A cocktail of inhibitors for equilibrative (ENT) and concentrative (CNT) nucleoside transporters (1 mM phloridzin, 100 μM dipyridamole, 10 μM NBMPR; [23-25]) was not able to significantly reduce adenosine-induced enhancement of beat frequency (Fig 2A; 26.3 ± 3.6%, P = 0.19), suggesting that neither influx nor efflux of adenosine analogs is responsible for adenosine's effect on beat frequency. Furthermore, selective (100 nM) concentrations of the adenosine receptor agonists CGS 21680 (A_{2A}; 2.7 ± 1.2%,), 2'MeCCPA (A_1; 0.9 ± 3.4%,), or IB-MECA (A_3; -1.0 ± 2.5%) did not reveal any enhancement of beat frequency (Fig. 2B) when compared to a no drug control (-0.1 ± 2.4%). Loss of subtype selectivity precluded the use of higher concentrations of these agonists for receptor identification. As a selective A_{2B} receptor agonist was not commercially available [26], we tested two selective A_{2B} receptor antagonists for their ability to block the NECA-induced enhancement of frequency. As shown in Fig. 2C, MRS 1754 (100 nM; 7.1 ± 2.7%) and PSB 603 (1 μM; 1.3 ± 2.0%) significantly blocked the increase in frequency induced by 1 μM NECA. Furthermore, enhancement of beat frequency by 300 μM BzATP was also significantly reduced by MRS 1754 application (Fig. 2C; 12.4 ± 2.0%), demonstrating that the previously observed BzATP response is primarily due to A_{2B} receptor activation. A residual $P2X_7$-mediated component cannot, however, be excluded.

In Ca^{2+} imaging experiments, focal applications of 1 μM NECA or 30 μM adenosine onto ependymal cells did not induce a change in $[Ca^{2+}]_i$, thus suggesting that A_{2B}-mediated enhancement of beat frequency is not Ca^{2+}-mediated (Fig. 2D). Separate beat frequency experiments demonstrated that 100 μM adenosine induces ciliary beat frequency enhancement in EGTA (ethylene glycol-bis(2-aminoethylether)-N, N, N', N'-tetraacetic acid)-buffered Ca^{2+}-free external solution (46.4 ± 8.2%, n = 2 slices, P < 0.05, data not shown), thereby supporting the conclusion that A_{2B}-mediated enhancement of beat frequency is not Ca^{2+}-mediated. Finally, as a positive control (and consistent with prior observations from our laboratory [17]), 300 μM BzATP-induces a dramatic increase in $[Ca^{2+}]_i$ (Fig. 2D).

Histochemical and functional evidence for A_{2B} expression: immunocytochemistry and $A_{2B}^{-/-}$/β-gal reporter gene knock-in mice

We next sought to confirm A_{2B} expression by ependymal cells using immunocytochemical methods. While distinct A_{2B} immunoreactivity was observed in ependymal cells (Fig. 3A), non-selective nuclear staining was also observed throughout the central nervous system (CNS) and therefore precluded definitive interpretation. Two additional A_{2B} antibodies did not show any CNS labeling (data not shown). A_{2A} immunoreactivity was evident in the striatum and in a scattered distribution along the SVZ but not in ependymal cells (Fig. 3B). An alternative approach was therefore used as a verification of the presence of A_{2B} receptors.

Previously characterized $A_{2B}^{-/-}$/β-gal reporter gene knock-in mice [19] were surveyed for A_{2B} gene promoter-driven expression of β-galactosidase in ependymal cells along the lateral ventricle. Strong X-gal reaction product was observed in the lateral septal nucleus, and clear intracellular labeling was also visible in ependymal cells and scattered throughout the cortex and striatum (Fig. 3C). This pattern was observed in $A_{2B}^{-/-}$/β-gal mice but not in wild-type controls. β-gal immunoreactivity was also observed in the $A_{2B}^{-/-}$/β-gal mice in S100β-positive ependymal cells (Fig. 3D-F), providing an additional layer of evidence for A_{2B} expression by ependyma. Ependymal X-gal reaction product is also visible in the corresponding Fig. 3G.

Functional evidence for A_{2B} expression by ependymal cells was also observed in the $A_{2B}^{-/-}$/β-gal mice (Fig. 4). Neither NECA (1 μM; -1.3 ± 1.8%) nor adenosine (30 μM; 4.0 ± 1.9%) was capable of increasing ciliary beat frequency in the $A_{2B}^{-/-}$/β-gal mice (Fig. 4A). BzATP, however, induces a significant (Fig. 4B), albeit smaller, enhancement of beat frequency in $A_{2B}^{-/-}$/β-gal mice (36.6 ± 3.0%) versus wild-type controls (58.9 ± 3.4%, data also in Fig. 1C). The increase induced by BzATP in the $A_{2B}^{-/-}$/β-gal mice is completely blocked by pre-incubation with the $P2X_7$ antagonist BBG (Fig. 4B; 0.8 ± 2.2%), thus providing additional evidence for a residual $P2X_7$-mediated enhancement in these animals. A summary diagram is presented in Fig. 4C.

Discussion

The present experiments demonstrated that activation of the adenosine A_{2B} receptor enhanced ciliary beat frequency in mouse lateral ventricle ependymal cells - a conclusion supported by pharmacological experiments using

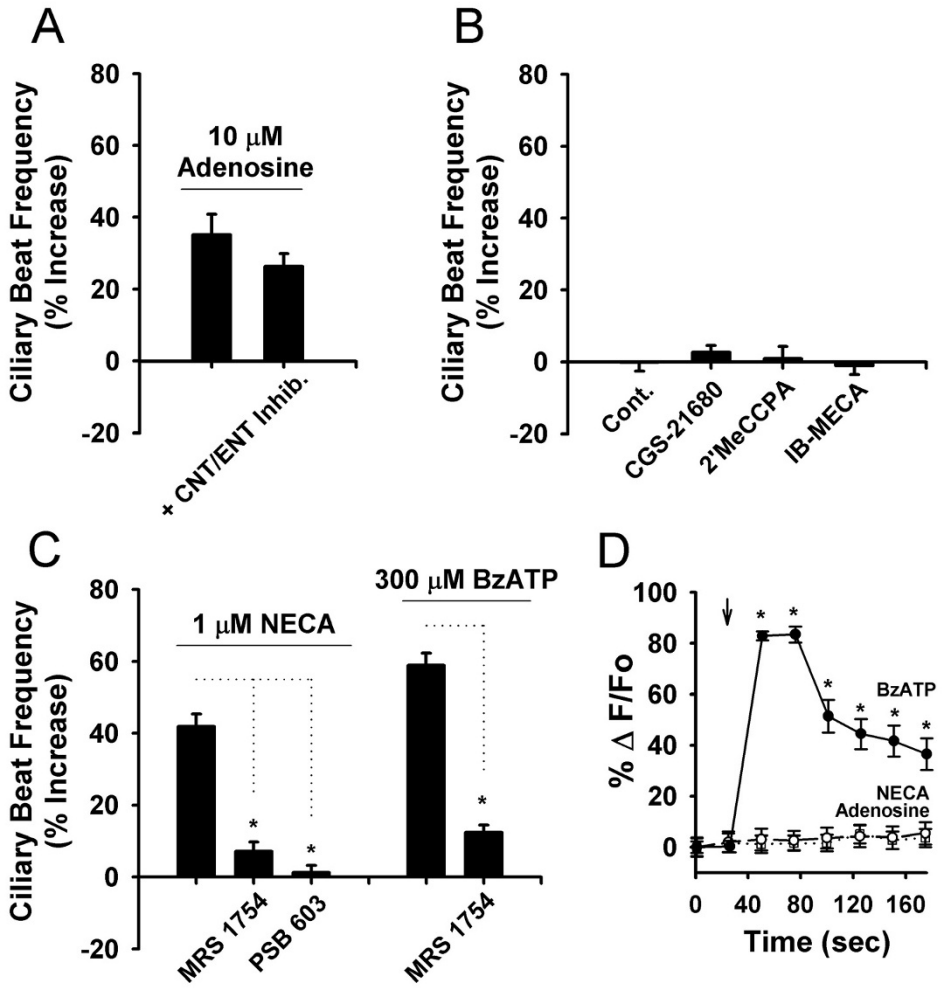

Figure 2

Adenosine-mediated enhancement of ciliary beat frequency is due to A2B receptor activation. (***A***) Histogram showing that ciliary beat frequency enhancement was not eliminated by pre-incubation with a cocktail of CNT and ENT inhibitors (1 mM phloridzin, 100 μM dipyridamole, 10 μM NBMPR; n = 5). (***B***) Summary histogram showing that ciliary beat frequency did not increase in response to a no drug control (Cont., n = 10), nor selective concentrations of the A_{2A} agonist CGS 21680 (100 nM, n = 5), the A_1 agonist 2'MeCCPA (100 nM, n = 5), nor the A_3 agonist IB-MECA (100 nM, n = 5). There was no significant difference between the no drug control and CGS 21680, 2'MeCCPA, or IB-MECA. (***C***) Histogram demonstrating that the response to 1 μM NECA was significantly reduced by the A_{2B} antagonist MRS 1754 (100 nM, n = 9) and eliminated by the A_{2B} antagonist PSB 603 (1 μM, n = 10). Response to 300 μM BzATP was also reduced by MRS 1754 (100 nM, n = 8). (***D***) $[Ca^{2+}]_i$ was increased by 1 min focal application (↓) of 300 μM BzATP ([Black circle], n = 1 application/10 regions of interest), but not by 3 min applications of 1 μM NECA (❍, n = 3 applications/30 regions of interest) or 30 μM adenosine, (□, n = 3 applications/30 regions of interest): note: ❍ and □ symbols largely overlap. The percent change in fluorescence signal divided by baseline mean fluorescence intensity is shown in the Y-axis (%$\Delta F/F_0$). *: $P < 0.05$ for all panels, data are means ± SEM. The ***n*** value indicates the number of slices tested.

selective adenosine receptor agonists and antagonists, as well as experiments using the $A_{2B}^{-/-}$/β-gal mice. The fact that BzATP application onto mouse brain slices can lead to activation of a non-$P2X_7$-mediated pathway is not surprising. For example, prior studies in the hippocampus have demonstrated that BzATP can induce non-$P2X_7$-mediated effects through the action of ecto-nucleotidases, nucleoside transporters, and subsequent adenosine receptor activation [27]. Ependymal cells have been shown to express ecto-nucleotide pyrophasphatase/phosphodiesterase 1 (NPP1) and ecto-5'-nucleotidase [28,29], and the decrease in BzATP-mediated effects after pre-incubation with αβmADP (an ecto-5'-nucleotidase inhibitor; Fig. 1C) suggests that ciliary beat frequency enhancement is

largely dependent on a metabolic breakdown product rather than BzATP itself.

It should be noted that BBG was used as the sole $P2X_7$ antagonist in these studies, as the more commonly used adenosine 5'triphosphate-2',3'-dialdehyde (oATP) induced toxicity in prior experiments (unpublished observations) and KN-62 has demonstrated a weaker activity at mouse versus human $P2X_7$ receptors [30]. Our recent whole-cell patch clamp experiments, however, showed clear antagonism of ependymal cell BzATP-induced currents by low concentrations of BBG [17]. Furthermore, no additional P2X receptor subtypes were detected during patch clamp recordings of $P2X_7^{-/-}$ mice [17]. While data in Fig. 1C, Fig. 2C, and Fig. 4B argue that a minor $P2X_7$-mediated component to BzATP-induced ciliary beat frequency enhancement is present, it is most easily observed in the absence of the adenosine A_{2B} receptor (Fig. 4B).

The lack of ciliary beat frequency enhancement with 100 μM UTP (Fig. 1D), and the absence of a suramin-mediated antagonism of ATP-induced changes in beat frequency (Fig. 1D), strongly argue against a P2Y-mediated modulation of frequency in the present experiments. These data do not altogether eliminate the possibility, however, that another subtype of P2Y-receptor may play a role in beat frequency modulation. A more extensive pharmacological analysis (with inclusion of appropriate ecto-nucleotidase inhibitors to prevent breakdown of purinergic drugs into adenosine receptor agonists) is clearly desirable and should be the focus of future investigation.

Interestingly, ATP has previously been shown to decrease ciliary beat frequency in rat 4th ventricle ependymal cells [14]. It is reasonable to assume that species and region-specific differences may exist in ependymal cell response to ATP, which is obviously dependent on the subtypes of purinergic receptors expressed. For example, in our mouse lateral ventricle ependymal cells, $[Ca^{2+}]_i$ increases rapidly after BzATP application (Fig. 2D and [17]); this is in sharp contrast to ATP's lack of $[Ca^{2+}]_i$ effect in the previously mentioned rat experiments [14]. Other proteins expressed by ependyma during development - such as glial fibrillary acidic protein (GFAP) and vimentin - vary markedly between species, developmental stage, and location along the ventricular system [31]. Future work on anatomic as

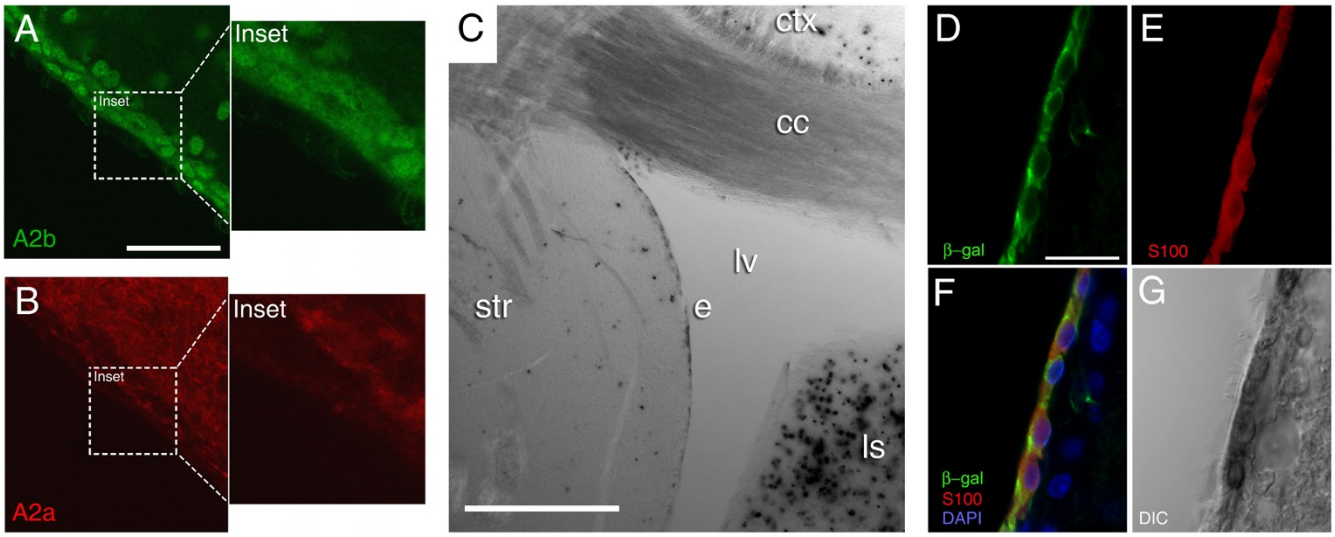

Figure 3

Ependymal localization of A_{2B}: evidence from immunocytochemistry and X-gal staining. (*A*) Cytoplasmic A_{2B}-immunoreactivity was evident in ependymal cells (see inset) of wild type mice, although non-specific nuclear labeling was also evident throughout the brain and confounds interpretation of ependymal immunoreactivity. (*B*) No labeling of ependymal cells was observed using an antibody to A_{2A} receptors in wild type mice, although strong immunoreactivity was evident in the striatum and in a scattered distribution along the SVZ. (*C*) DIC image from an $A_{2B}^{-/-}$/β-gal reporter gene knock-in mouse showing darkening of cells due to X-gal precipitate in regions surrounding the ependymal layer (e). Strong X-gal labeling was observed in the lateral septal nucleus (*ls*), while scattered labeling was observed in the striatum (*st*) and cortex (*ctx*) but not in the corpus callosum (*cc*). The septum mechanically separated from the corpus callosum during the staining procedure, thus obliterating the dorso-medial boundary of the lateral ventricle (*lv*) in this slice. (Bar = 500 μm). (*D-F*) Immunocytochemistry from an $A_{2B}^{-/-}$/β-gal reporter gene knock-in mouse demonstrating that β-galactosidase (*D*; green, Bar = 25 μm) and S100β (*E*, red) are co-localized in ependymal cells (*F*). Nuclei are stained with DAPI (blue). (*G*) Corresponding DIC image with darkening of the ependyma due to X-gal precipitate.

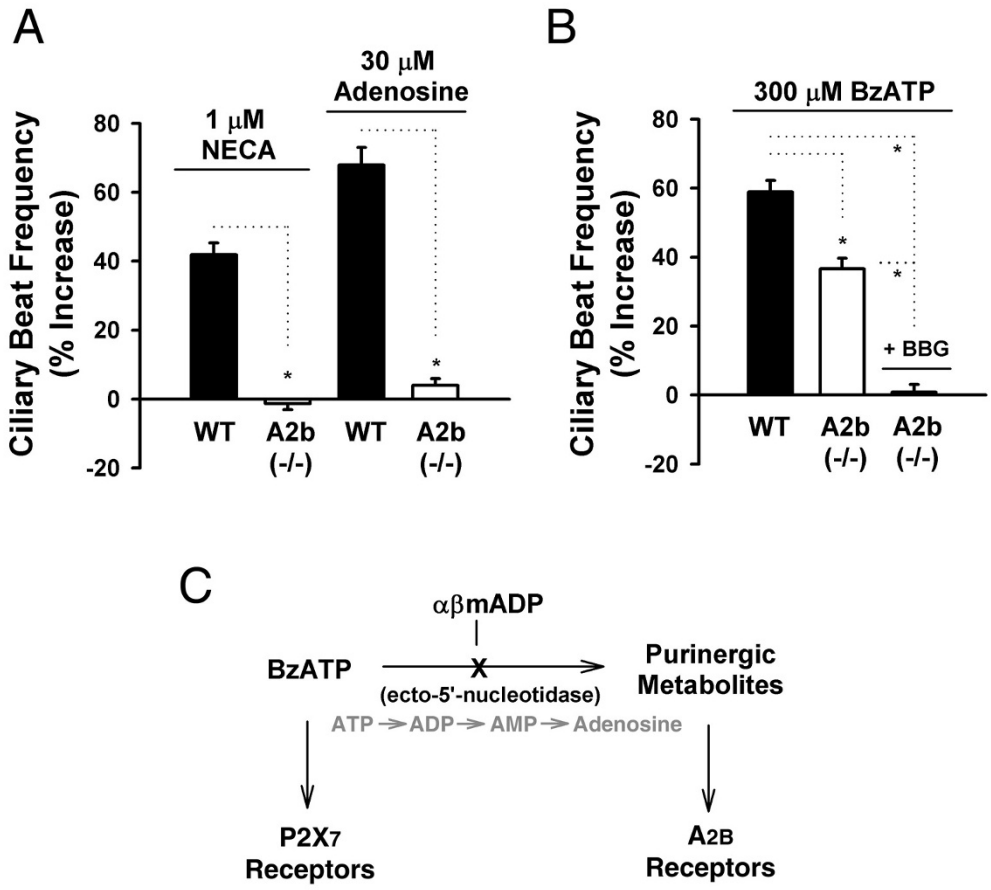

Figure 4

Ciliary beat frequency analysis in $A_{2B}^{-/-}$/β-gal reporter gene knock-in mice. (*A*) Histogram showing the absence of ciliary beat frequency enhancement due to 1 μM NECA (n = 10) and 30 μM adenosine (n = 10) in the $A_{2B}^{-/-}$ mice. (*B*) Enhancement due to 300 μM BzATP application was reduced in the $A_{2B}^{-/-}$ mice (n = 8) versus wild-type $P2X_7^{+/+}$ mice (n = 5). BzATP-induced enhancement was eliminated in the $A_{2B}^{-/-}$ mice after pre-incubation of the slices with 100 nM BBG (n = 8). *: $P < 0.05$ for all panels, data are means ± SEM. The *n* value indicates the number of slices tested. (*C*) Summary diagram showing enzymatic breakdown of BzATP and subsequent receptor activation. ATP (an endogenous signaling molecule analogous to BzATP) is shown in grey.

well as species-specific differences in ependymal cell ciliary beat frequency regulation is clearly warranted.

A_{2B} can be coupled to multiple G-protein cascades, including the adenylate cyclase (Gs; cAMP) pathway and the phospholipase C (Gq11) signaling pathways [32-35]. Furthermore, activation of the phospholipase C - mediated pathway can lead to $[Ca^{2+}]_i$ increases after A_{2B} activation [32]. In the present experiments, however, neither NECA (1 μM) nor adenosine (30 μM) were able to induce $[Ca^{2+}]_i$ increases in ependymal cells (Fig. 2D), arguing against a Ca^{2+}-mediated mechanism for A_{2B}-induced enhancement of ciliary beat frequency. While additional pathways involved in A_{2B}-mediated signaling were not explored in the present experiments, a complete understanding of these pathways may prove critical for determining the importance of receptor signaling cascades in CSF dynamics. For example, a recent study by Mönkkönen *et al*. (2007) has demonstrated that knockdown of $G_{\alpha i2}$ can lead to ciliary stasis and ventricular dilation [11].

Nucleotide signaling and purinergic receptor expression in the developing brain has been the subject of intense investigation (for review, see [36]). For example, the developmental precursors of ependyma - radial glia [37] - can propagate ATP-mediated Ca^{2+} waves that are dependent on $P2Y_1$ receptor expression [38]. Immature ependyma are born between embryonic days E14 and E16 in the mouse, although cell maturation and cilia formation typically occur during the first postnatal week [37]. Little is

known regarding the functional role of purinergic receptors on these cells during this time. It should also be noted that neuroblast migration from the SVZ to the rostral migratory stream depends on the normal flow of CSF, and ciliary motility is required for maintaining a diffusional gradient of inhibitory guidance molecules in the CSF [39]. Whether receptor-mediated changes in ciliary beat frequency play a role in this phenomenon is not known. Purinergic receptor expression on CSF secreting cells of the choroid plexus has also been the subject of recent investigations [40,41].

Additional questions clearly remain to be answered. Is the source of endogenous ATP or adenosine autocrine or paracrine? Does ciliary beat frequency correlate with the metabolic requirements in the CNS, and might ciliary beat frequency dysregulation be associated with hydrocephalus? While answers to these questions are beyond the scope of the present experiments, much remains to be learned about the role of purinergic receptors and ciliary beat frequency in cerebral fluid dynamics.

Conclusion

While abnormal ciliary structure and function has been associated with hydrocephalus in several experimental models, the signaling mechanisms responsible for the normal regulation of ependymal cell ciliary beat frequency are not well understood. The present experiments demonstrate that activation of the adenosine A_{2B} receptor enhances ciliary beat frequency in lateral ventricle ependymal cells. A residual contribution of purinergic $P2X_7$ receptors to frequency regulation is also supported. Purinergic modulation of ependymal cell beat frequency may play an important role in maintaining normal fluid balance in the CNS. Future experiments should focus on understanding whether purinergic dysregulation contributes to pathologic conditions such as hydrocephalus.

Abbreviations

aCSF: artificial cerebrospinal fluid; **αβmADP**: adenosine 5'-(α,β-methylene)diphosphate; **ATP**: adenosine 5'-triphosphate; **BBG**: brilliant blue G; **β-gal**: β-galactosidase; **BzATP**: 2'(3')-*O*-(4-benzoylbenzoyl)adenosine 5'-triphosphate triethylammonium salt; **cAMP**: adenosine 3',5'-cyclic monophosphate; **CGS-21680**: 4-[2-[[6-Amino-9-(*N*-ethyl-b-D-ribofuranuronamidosyl)-9*H*-purin-2-yl]amino]ethyl]benzenepropanoic acid hydrochloride; **CNT**: concentrative nucleoside transporter; **DAPI**: (2-(4-Amidinophenyl)-6-indolecarbamidine dihydrochloride); **DIC**: differential interference contrast; **DMSO**: dimethyl sulfoxide; **ENT**: equilibrative nucleoside transporter; **IB-MECA**: 1-deoxy-1-[6-[[(3-iodophenyl)methyl]amino]-9*H*-purin-9-y l]-*N*-methyl-b-D-ribofuranuronamide; **2'MeCCPA**: 2-chloro-*N*-cyclopentyl-2'-methyladenosine; **MRS 1754**: *N*-(4-cyanophenyl)-2-[4-(2,3,6,7-tetrahydro-2,6-dioxo-1,3-dipropyl-1*H*-purin-8-yl)phenoxy]-acetamide; **NBMPR**: S-(4-Nitrobenzyl)-6-thioinosine; **NECA**: 5'-*N*-ethylcarboxamidoadenosine; **NPP1**: ecto-nucleotide pyrophasphatase/phosphodiesterase 1; **oATP**: adenosine 5'triphosphate-2',3'-dialdehyde; **PBS**: phosphate buffered saline; **PSB 603**: 8-[4-[4-(4-chlorophenzyl)piperazide-1-sulfonyl)phenyl]]-1-propylxanthine; **SVZ**: subventricular zone; **TBS**: Tris buffered saline; **TBST**: TBS + 0.1% Triton X-100; **UTP:** uridine 5'-triphosphate.

Competing interests

The authors declare that they have no competing interests.

Authors' contributions

JRG. and AB designed research; JRG performed ciliary beat frequency, immunocytochemistry, and calcium imaging experiments at Yale University; KR and DY developed the A2b KO mouse at Boston University; DY performed X-gal staining; JRG analyzed data and wrote the manuscript. All authors have read and approved the final version of the manuscript.

Acknowledgements

The β-galactosidase antibody was provided by Dr. Marion Richard in the laboratory of Dr. Charles A. Greer. Dr. Jean-Claude Platel provided technical assistance with histochemistry and calcium imaging. Dr. Oliver Henschel provided advice on ImageJ analysis. This work was supported by grants from the National Institute of Health R01 NS048256 and DC007681 (AB) and 2T32HL007974-05 (JRG).

References

1. Del Bigio MR: **The ependyma: a protective barrier between brain and cerebrospinal fluid.** *Glia* 1995, **14:**1-13.
2. Yamadori T, Nara K: **The directions of ciliary beat on the wall of the lateral ventricle and the currents of the cerebrospinal fluid in the brain ventricles.** *Scan Electron Microsc* 1979, **3:**335-340.
3. Lechtreck KF, Delmotte P, Robinson ML, Sanderson MJ, Witman GB: **Mutations in Hydin impair ciliary motility in mice.** *J Cell Biol* 2008, **180:**633-643.
4. Lee L, Campagna DR, Pinkus JL, Mulhern H, Wyatt TA, Sisson JH, Pavlik JA, Pinkus GS, Fleming MD: **Primary ciliary dyskinesia in mice lacking the novel ciliary protein Pcdp1.** *Mol Cell Biol* 2008, **28:**949-957.
5. Banizs B, Pike MM, Millican CL, Ferguson WB, Komlosi P, Sheetz J, Bell PD, Schwiebert EM, Yoder BK: **Dysfunctional cilia lead to altered ependyma and choroid plexus function, and result in the formation of hydrocephalus.** *Development* 2005, **132:**5329-5339.
6. Kosaki K, Ikeda K, Miyakoshi K, Ueno M, Kosaki R, Takahashi D, Tanaka M, Torikata C, Yoshimura Y, Takahashi T: **Absent inner dynein arms in a fetus with familial hydrocephalus-situs abnormality.** *Am J Med Genet A* 2004, **129A:**308-311.
7. Takaki E, Fujimoto M, Nakahari T, Yonemura S, Miyata Y, Hayashida N, Yamamoto K, Vallee RB, Mikuriya T, Sugahara K, Yamashita H, Inouye S, Nakai A: **Heat shock transcription factor 1 is required for maintenance of ciliary beating in mice.** *J Biol Chem* 2007, **282:**37285-37292.
8. Ibanez-Tallon I, Pagenstecher A, Fliegauf M, Olbrich H, Kispert A, Ketelsen UP, North A, Heintz N, Omran H: **Dysfunction of axonemal dynein heavy chain Mdnah5 inhibits ependymal flow and reveals a novel mechanism for hydrocephalus formation.** *Hum Mol Genet* 2004, **13:**2133-2141.

9. Fernandez-Gonzalez A, Kourembanas S, Wyatt TA, Mitsialis SA: **Mutation of murine adenylate kinase 7 underlies a primary ciliary dyskinesia phenotype.** *Am J Respir Cell Mol Biol* 2009, **40:**305-313.
10. Bush A, Chodhari R, Collins N, Copeland F, Hall P, Harcourt J, Hariri M, Hogg C, Lucas J, Mitchison HM, O'Callaghan C, Phillips G: **Primary ciliary dyskinesia: current state of the art.** *Arch Dis Child* 2007, **92:**1136-1140.
11. Monkkonen KS, Hakumaki JM, Hirst RA, Miettinen RA, O'Callaghan C, Mannisto PT, Laitinen JT: **Intracerebroventricular antisense knockdown of G alpha i2 results in ciliary stasis and ventricular dilatation in the rat.** *BMC Neurosci* 2007, **8:**26.
12. Domínguez-Pinos MD, Páez P, Jiménez AJ, Weil B, Arráez M-A, Pérez-Fígares J-M, Rodríguez E-M: **Ependymal denudation and alterations of the subventricular zone occur in human fetuses with a moderate communicating hydrocephalus.** *J Neuropathol Exp Neurol* 2005, **64:**595-604.
13. Nelson DJ, Wright EM: **The distribution, activity, and function of the cilia in the frog brain.** *J Physiol* 1974, **243:**63-78.
14. Nguyen T, Chin WC, O'Brien JA, Verdugo P, Berger AJ: **Intracellular pathways regulating ciliary beating of rat brain ependymal cells.** *J Physiol* 2001, **531:**131-140.
15. Hirst RA, Sikand KS, Rutman A, Mitchell TJ, Andrew PW, O'Callaghan C: **Relative roles of pneumolysin and hydrogen peroxide from Streptococcus pneumoniae in inhibition of ependymal ciliary beat frequency.** *Infect Immun* 2000, **68:**1557-1562.
16. Hirst RA, Kadioglu A, O'Callaghan C, Andrew PW: **The role of pneumolysin in pneumococcal pneumonia and meningitis.** *Clin Exp Immunol* 2004, **138:**195-201.
17. Genzen JR, Platel JC, Rubio ME, Bordey A: **Ependymal cells along the lateral ventricle express functional P2X(7) receptors.** *Purinergic Signal* 2009, **5:**299-307.
18. Solle M, Labasi J, Perregaux DG, Stam E, Petrushova N, Koller BH, Griffiths RJ, Gabel CA: **Altered cytokine production in mice lacking P2X(7) receptors.** *J Biol Chem* 2001, **276:**125-132.
19. Yang D, Zhang Y, Nguyen HG, Koupenova M, Chauhan AK, Makitalo M, Jones MR, St Hilaire C, Seldin DC, Toselli P, Lamperti E, Schreiber BM, Gavras H, Wagner DD, Ravid K: **The A2B adenosine receptor protects against inflammation and excessive vascular adhesion.** *J Clin Invest* 2006, **116:**1913-1923.
20. Platel JC, Dupuis A, Boisseau S, Villaz M, Albrieux M, Brocard J: **Synchrony of spontaneous calcium activity in mouse neocortex before synaptogenesis.** *Eur J Neurosci* 2007, **25:**920-928.
21. Yang D, Koupenova M, McCrann DJ, Kopeikina KJ, Kagan HM, Schreiber BM, Ravid K: **The A2b adenosine receptor protects against vascular injury.** *PNAS* 2008, **105:**792-796.
22. Naito Y, Lowenstein JM: **5'-Nucleotidase from rat heart membranes. Inhibition by adenine nucleotides and related compounds.** *Biochem J* 1985, **226:**645-651.
23. Hirsh AJ, Stonebraker JR, van Heusden CA, Lazarowski ER, Boucher RC, Picher M: **Adenosine deaminase 1 and concentrative nucleoside transporters 2 and 3 regulate adenosine on the apical surface of human airway epithelia: implications for inflammatory lung diseases.** *Biochemistry* 2007, **46:**10373-10383.
24. Kiss A, Farah K, Kim J, Garriock RJ, Drysdale TA, Hammond JR: **Molecular cloning and functional characterization of inhibitor-sensitive (mENT1) and inhibitor-resistant (mENT2) equilibrative nucleoside transporters from mouse brain.** *Biochem J* 2000, **352(Pt 2):**363-372.
25. Ward JL, Sherali A, Mo ZP, Tse CM: **Kinetic and pharmacological properties of cloned human equilibrative nucleoside transporters, ENT1 and ENT2, stably expressed in nucleoside transporter-deficient PK15 cells. Ent2 exhibits a low affinity for guanosine and cytidine but a high affinity for inosine.** *J Biol Chem* 2000, **275:**8375-8381.
26. Baraldi PG, Tabrizi MA, Fruttarolo F, Romagnoli R, Preti D: **Recent improvements in the development of A(2B) adenosine receptor agonists.** *Purinergic Signal* 2009, **5:**3-19.
27. Kukley M, Stausberg P, Adelmann G, Chessell IP, Dietrich D: **Ecto-nucleotidases and nucleoside transporters mediate activation of adenosine receptors on hippocampal mossy fibers by P2X7 receptor agonist 2'-3'-O-(4-benzoylbenzoyl)-ATP.** *J Neurosci* 2004, **24:**7128-7139.
28. Bjelobaba I, Nedeljkovic N, Subasic S, Lavrnja I, Pekovic S, Stojkov D, Rakic L, Stojiljkovic M: **Immunolocalization of ecto-nucleotide pyrophosphatase/phosphodiesterase 1 (NPP1) in the rat forebrain.** *Brain Res* 2006, **1120:**54-63.
29. Braun N, Brendel P, Zimmermann H: **Distribution of 5'-nucleotidase in the developing mouse retina.** *Brain Res Dev Brain Res* 1995, **88:**79-86.
30. Hibell AD, Thompson KM, Simon J, Xing M, Humphrey PP, Michel AD: **Species- and agonist-dependent differences in the deactivation-kinetics of P2X7 receptors.** *Naunyn Schmiedebergs Arch Pharmacol* 2001, **363:**639-648.
31. Sarnat HB: **Histochemistry and immunohistochemistry of the developing ependyma and choroid plexus.** *Microsc Res Tech* 1998, **41:**14-28.
32. Panjehpour M, Castro M, Klotz KN: **Human breast cancer cell line MDA-MB-231 expresses endogenous A2B adenosine receptors mediating a Ca2+ signal.** *Br J Pharmacol* 2005, **145:**211-218.
33. Foektistov I, Biaggioni I: **Adenosine A2b receptors evoke interleukin-8 secretion in human mast cells. An enprofylline-sensitive mechanism with implications for asthma.** *J Clin Invest* 1995, **96:**1979-1986.
34. Fredholm BB, AP IJ, Jacobson KA, Klotz KN, Linden J: **International Union of Pharmacology. XXV. Nomenclature and classification of adenosine receptors.** *Pharmacol Rev* 2001, **53:**527-552.
35. Linden J, Thai T, Figler H, Jin X, Robeva AS: **Characterization of human A2B adeosine receptors: radioligand binding, western blotting, and coupling to Gq in human embryonic kidney 293 cells and HMC-1 mast cells.** *Molec Pharm* 1999, **56:**705-713.
36. Zimmermann H: **Nucleotide signaling in nervous system development.** *Pflugers Arch* 2006, **452:**573-588.
37. Spassky N, Merkle FT, Flames N, Tramontin AD, García-Verdugo JM, Alvarez-Buylla A: **Adult ependymal cells are postmitotic and are derived from radial glial cells during embryogenesis.** *J Neurosci* 2005, **25:**10-18.
38. Weissman TA, Riquelme PA, Ivic L, Flint AC, Kriegstein AR: **Calcium waves propagate through radial glial cells and modulate proliferation in the developing neocortex.** *Neuron* 2004, **43:**647-661.
39. Sawamoto K, Wichterle H, Gonzalez-Perez O, Cholfin JA, Yamada M, Spassky N, Murcia NS, Garcia-Verdugo JM, Marin O, Rubenstein JL, Tessier-Lavigne M, Okano H, Alvarez-Buylla A: **New neurons follow the flow of cerebrospinal fluid in the adult brain.** *Science* 2006, **311:**629-632.
40. Johansson PA, Burnstock G, Dziegielewska KM, Guida E, McIntyre P, Saunders NR: **Expression and localization of P2 nucleotide receptor subtypes during development of the lateral ventricular choroid plexus of the rat.** *Eur J Neurosci* 2007, **25:**3319-3331.
41. Xiang Z, Burnstock G: **Expression of P2X receptors in rat choroid plexus.** *Neuroreport* 2005, **16:**903-907.